

EVALUATION OF EXCAVATOR ENERGY CONSUMPTION AND OVERBURDEN CUTTING RESISTANCE USING MULTIPLE LINEAR REGRESSION

J. Trivan¹, S. Kostić^{2#}

¹University of Banja Luka, Faculty of Mining, Prijedor, Republic of Srpska, Bosnia and Herzegovina

²Jaroslav Černi Water Institute, Geology Department, Belgrade, Serbia

Received: March 15, 2022; Accepted: October 20, 2022

Abstract

In present paper the energy consumption of the excavator and overburden linear cutting resistance by invoking the multiple linear regression was examined. As a result, the corresponding models as nonlinear functions of physical and mechanical overburden properties: grain size, unit weight, cohesion, and friction angle, were proposed. The analysis was based on records made at "Tamnava Eastern Field" mine for the bucket-wheel excavator with new excavation teeth. The obtained results indicated that excavator energy consumption significantly depended on the grain size and cohesion, as individual factors, while the effect of two-factor interactions was particularly significant: clay percentage with cohesion and small grained sand fraction, and friction angle with medium grained sand and cohesion. On the other hand, linear cutting resistance of the overburden was largely controlled by all the examined physical and mechanical properties (grain size, unit weight, and shear strength), with the following significant two-factors interactions: shear strength parameters with all grain size fractions, different grain size fractions among each other, and friction angle with unit weight.

Key words: cutting resistance, energy consumption, unit weight, grain size, shear strength, multiple linear regression.

1. Introduction

Bucket-wheel excavator together with conveyors represents a part of continuous mining system used for coal exploitation in surface or open pit cast mining. Considering high costs of the replacing parts and significant losses when exploitation system is out of function, it is of primary importance to preserve the continuous operation and to prevent any sudden and unforeseen interruptions. These unexpected stoppages are commonly caused by the deformation of the excavator itself, due to the excavator age or due to inadequate assessment of the working environment. Therefore, modelling the overburden excavation process is of particular significance in surface mining since expenses in case of unplanned repair of excavation equipment could overcome the annual budget predicted for the specific activity. Good example of this is given by Ulbrich et al. [1], according to whom emergency renewal of bucket teeth caused by abrasive wear in American copper mines cost the mine 13.8 times more than a planned renewal of the same. Main reason for the

increased wear of the excavation teeth lies in inadequate characterization of the excavation environment, which is commonly conducted by field sampling and laboratory testing, after which test results are extrapolated to the whole corresponding unit in the field. Such procedure omits two important steps: sufficient frequency of sampling and adequate extrapolation of the test results to the whole geotechnical unit. Sufficient frequency of sampling secures that variability of the target geotechnical properties is covered, while, at the same time, extrapolation of test results is easier in case when sampling is done with satisfying frequency. Nevertheless, one needs to note that considering the size of surface mine, frequent sampling is almost never justified, so one needs to invoke specialized statistical techniques in order to examine the physically possible and statistically significant correlations among different parameters affecting the excavation process. This could be achieved using different regression techniques, including multiple linear regression [2] and nonlinear regression [3], or some of the methods from the bundle

#Corresponding author: srdjan.kostic@jcerni.rs

of artificial intelligence package, such as artificial neural networks [4], machine learning [5], or various hybrid techniques [6].

There are only few previous research studies that examine the resistance of overburden to excavation in surface mines. According to Trivan [7], Vetrov in 1965 first analyzed how several parameters affect the cutting force, primarily the physical and mechanical properties of the working environment, the geometry of cutting tools (inclination of the rotor to the rotor boom, the position of the teeth on the buckets and the inclination of the rotor) and wear tools. Dombrovski in 1972 performed field experiments with excavator buckets, and based on the research results, it was concluded that digging resistance depends on the geometric parameters of cuts, physical and mechanical properties of the working environment, and the shape and dimensions of the working tool [7]. Coleman and Fitzhardinge [8] established a correlation between compressive strength, chisel cutting resistance, and point load strength index. Inal [9] developed a new digging resistance index for tooth excavators, based on the correlation between rock compressive strength and cutting force. Based on research from surface mines in Poland, Szepliatowski, in 1991, defined the specific resistance of digging as a function of cohesion, bulk density and looseness, including the bucket and tooth types [7]. Scheffler [10] analyzed the possibility of predicting the cutting resistance on excavators with teeth under the influence of rock structure parameters. Razz [11] considered the influence of the working environment on the cutting force using the point-load test and the original software for the optimal choice of technological parameters of the working process and tooth geometry. Su and Akcin [12], proposed a relationship between the Shore hardness index and several properties of coal: uniaxial compressive strength, Shore hardness index, dynamic strength index, and cone penetration values. Amar et al. [13], introduced the resistance index as a function of several numerical indicators associated with the qualitative properties of rock mass (estimates of point strength index, abrasiveness estimates, volumetric cracking coefficient, influence of blade orientation in relation to the position of main discontinuities in rock mass and applied forces of mechanization). Langham-Williams and Hagan [14] proposed some simple correlations between uniaxial compressive strength of several rock types (sandstone, gravel, coal, conglomerates and injection mass) and their cutting properties (specific

energy, cutting force and normal force).

Research presented in this paper represents further extension of the previous research [15], where an optimization of overburden excavation process was proposed, by providing explicit mathematical expressions for estimation of the maximum current consumption and wheel velocity depending on the overburden geomechanical properties. In present paper, the models for estimation of maximum energy consumption and cutting resistance considering the effect of grain size, unit weight and shear strength of overburden were further proposed.

Present paper is structured as follows. In Section 2 the analyzed dataset was described. In Section 3 the main results of the research were provided, while discussion and conclusions were given in Section 4.

2. Applied methodology and data analyzed

Data whose range is given in Tables 1 and 2 are examined by invoking the multiple linear regression (MLR) analysis, which commonly provides solutions of satisfying accuracy in area of regression between the possible influencing input factors and target outputs. Special attention is devoted to analysis of possible statistically significant two-factor interactions. Results of MLR approach are evaluated using ANOVA test, testing distribution of residuals, and by calculating the determination coefficient (R) and mean squared error (MSE).

In present paper, the data obtained from the overburden excavation at the "Tamnava Eastern field" open-pit coal mine in Serbia were analyzed [16]. At this coals site, lignite in the productive series is grouped mainly in three coal layers of higher thickness and several layers of low thickness in the underlying layer of the series. The top and bottom of the coal beds are made up of sediments from the upper Pontian, except in parts where the top sediments were eroded. The Upper Pontian sediments are developed into facies of clay, sandy and silty clays and sands, which alternate. Clay predominates in the eastern part of the basin, and sand in the western part. In the "Tamnava - East Field" surface mine, the bottom of the coal seam is represented by a layer of sand about 100 m thick. Above the sand is the main coal seam with a coal thickness of about 10-30 m. The overlying layer is made of silty clay with occurrences of lenses of fine-grained sands up to 28 m thick.

Data on E_{max} and KL_{max} were calculated using data

from the bucket-wheel excavator of type SchRs 900 25/6, as functions of maximum current consumption of the excavator (I_{max}), velocity of the excavator rotary movement (V_b), unit weight of the excavated material (γ), gravity acceleration (g), height of the material lift up to the dump location (h_d), rated voltage (U), power factor ($\cos\varphi$), cut height (h), cut thickness (s), coefficient of useful effect (η) power of unloaded motion (N_{pr}), total length of the cutting edges in contact with material, total area of cross-sections of the cut pieces and total number of buckets which are in the same time in contact with material [Trivan, 2022]. Characteristics of the bucket-wheel excavator were the following: installed engine power for rotary wheel $N_m=2 \times 230$ kW, geometric volume of bucket $q=0.9$ m³, number of buckets $z=14$, number of emptying buckets per minute $n=76$ min⁻¹, angular distance between buckets 0.4488 rad, diameter of rotary wheel $D=10.2$ m, length of rotary arrow $L_s=35$ m, perimeter velocity of rotary wheel $V_k=2.89$ m/s [16]. Ranges of the examined input and output factors are given in Tables 1 and 2. K_{Lmax} was determined in laboratory conditions, by applying Orenstein and Koppel method.

Table 1 Range of the obtained laboratory values for the examined influential factors: percentage of different grain size fractions, overburden unit weight and shear strength parameters

Influential factors	Range of laboratory determined values
CL_{per} percentage of clay in overburden (%)	5-45
SI_{per} percentage of silt in overburden (%)	43-91
SSN_{per} percentage of small-grained sand in overburden (%)	2-61
MSN_{per} percentage of moderate-grained sand in overburden (%)	1-8
γ unit weight of the overburden (kN/m ³)	16-22
c overburden cohesion (kPa)	19-25
φ overburden angle of internal friction (°)	22-23

Table 2 Range of the output parameters, maximum energy consumption E_{max} and maximum linear cutting resistance, K_{Lmax}

Output factors	Range of recorded values
Maximum energy consumption, E_{max} [kWh/m ³]	0.16-0.27
Maximum linear cutting force, K_{Lmax} [N/cm]	473-833

3. Results

Results of the performed analysis are shown in the following expressions:

$$E_{max} = 8.88414 - 0.018559 \cdot CL_{per} + 0.0018 \cdot SI_{per} + 0.0093 \cdot SSN_{per} - 0.50 \cdot MSN_{per} - 0.016339 \cdot G - 0.25688 \cdot c - 0.38393 \cdot \varphi + 0.00007 \cdot CL_{per} \cdot SSN_{per} + 0.0009 \cdot CL_{per} \cdot c + 0.0009 \cdot SI_{per} \cdot c - 0.00034 \cdot SSN_{per} \cdot c + 0.022 \cdot MSN_{per} \cdot \varphi + 0.012 \cdot c \cdot \varphi - 0.00006 \cdot CL_{per}^2 - 0.0002 \cdot SI_{per}^2 - 0.00005 \cdot SSN_{per}^2 + 0.0025 \cdot MSN_{per}^2 + 0.00051 \cdot G^2 - 0.0022 \cdot c^2 \quad (1)$$

$$K_{Lmax} = 32288.46 - 227.05 \cdot CL_{per} - 0.185 \cdot SI_{per} + 111.63 \cdot SSN_{per} - 2408.54 \cdot MSN_{per} - 1039.24 \cdot G - 113.22 \cdot c - 1155.62 \cdot \varphi - 0.42 \cdot CL_{per} \cdot SI_{per} + 0.41 \cdot CL_{per} \cdot SSN_{per} - 1.43 \cdot CL_{per} \cdot MSN_{per} + 2.27 \cdot CL_{per} \cdot G + 4.30 \cdot CL_{per} \cdot c + 6.49 \cdot CL_{per} \cdot \varphi - 3.28 \cdot SI_{per} \cdot MSN_{per} + 4.05 \cdot SI_{per} \cdot c - 1.75 \cdot SSN_{per} \cdot c - 2.88 \cdot SSN_{per} \cdot \varphi + 18.79 \cdot MSN_{per} \cdot c + 95.88 \cdot MSN_{per} \cdot \varphi + 29.77 \cdot G \cdot \varphi - 0.7 \cdot CL_{per}^2 - 0.43 \cdot SI_{per}^2 - 0.29 \cdot SSN_{per}^2 + 11.64 \cdot MSN_{per}^2 + 9.09 \cdot G^2 - 7.7 \cdot c^2 \quad (2)$$

where E_{max} stands for maximum energy consumption (KWh/m³), K_{Lmax} is the maximum linear cutting resistance (N/cm), CL_{per} , SI_{per} , SSN_{per} , MSN_{per} are percentage of clay, silt, small-grained sand and medium-grained sand, respectively; G stands for the unit weight of the overburden (kN/m³), c (kPa) and φ (°) are cohesion and angle of internal friction of the overburden. Table 3 represents the results of ANOVA tests for Eqs. (1) and (2).

Statistical analyzes indicated high value of determination coefficient and small values of MSE: $R=0.83$, $MSE=0.019$ (for Eq. 1) and $R=0.95$, $MSE=27.61$ (for Eq. 2). It is clear from normal plots of residuals in Figure 1 that error terms are normally distributed.

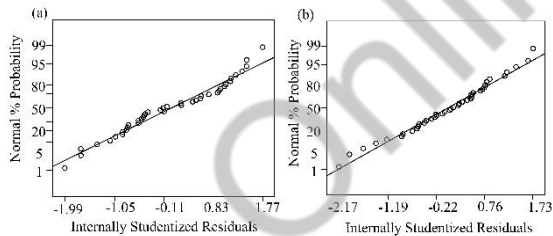
3.1. Maximum energy consumption

Regarding the parameter E_{max} , performed analyzes indicated significant influence of the following individual factors: small and medium grained sand, percentage of silt fraction and cohesion (Figure 2).

Table 3 Results of ANOVA tests for models (1) and (2)

Model (1)				Model (2)			
factors	Sum of squares	F value	P value	factors	Sum of squares	F value	P value
CL _{per}	7.1x10 ⁻⁴	1.02	0.32	CL _{per}	758.84	0.32	0.58
Sl _{per}	1.5x10 ⁻³	2.14	0.16	Sl _{per}	18065.62	7.70	0.02
SSN _{per}	8.2x10 ⁻⁷	1.2x10 ⁻³	0.97	SSN _{per}	1190.34	0.51	0.49
MSN _{per}	2.7x10 ⁻³	3.9	0.06	MSN _{per}	4497.67	1.92	0.19
G	4.2x10 ⁻⁴	0.6	0.44	G	33479.29	14.27	0.002
c	2.2x10 ⁻³	3.2	0.09	c	54810.09	23.36	0.0003
φ	1.6x10 ⁻³	2.3	0.15	φ	42853.56	18.26	0.0009
CL _{per} X SSN _{per}	2.9x10 ⁻³	4.2	0.05	CL _{per} X Sl _{per}	23131.81	9.86	0.0078
CL _{per} X c	5.3x10 ⁻³	7.7	0.01	CL _{per} X SSN _{per}	30573.31	13.03	0.0032
Sl _{per} X c	4.4x10 ⁻³	6.4	0.02	CL _{per} X G	26338.03	11.23	0.0052
MSN _{per} X φ	9.0x10 ⁻³	13.0	0.01	CL _{per} X c	46288.89	19.73	0.0007
c X φ	3.8x10 ⁻³	5.5	0.03	CL _{per} X φ	13021.91	5.55	0.0348
Sl _{per} ²	6.3x10 ⁻³	9.1	0.01	Sl _{per} X MSN _{per}	68118.68	29.03	0.0001
SSN _{per} ²	6.5x10 ⁻³	9.4	0.01	Sl _{per} X c	21847.88	9.31	0.0093
MSN _{per} ²	2.6x10 ⁻³	3.8	0.07	SSN _{per} X c	29239.86	12.46	0.0037
residual	0.014			SSN _{per} X φ	8408.81	3.58	0.0808

Model (2)				Model (2)			
factors	Sum of squares	F value	P value	factors	Sum of squares	F value	P value
MSN _{per} X c	43889.01	18.71	0.0008	Sl _{per} ²	17796.36	7.58	0.0164
MSN _{per} X φ	89812.51	38.28	<0.0001	SSN _{per} ²	71795.55	30.60	<0.0001
G X φ	17377.24	7.41	0.0175	MSN _{per} ²	17459.17	7.44	0.0173
CL _{per} ²	83787.77	35.71	<0.0001	G ²	20428.31	8.71	0.0113
				Residual	30501.40		

**Figure 1** Normal probability plots of residuals for Eq.1 (a) and Eq.2 (b)

As it could be seen from Figure 2, the only clear positive effect on E_{max} comes from MSN_{per} , i.e. with the increase of MSN_{per} , E_{max} increased as well, which could be explained by the increasing energy consumption due to increase in percentage of medium grained sand. On the other hand, one should note that the range of MSN_{per} was small (1-8%), so the obtained influence could have another form for a wider range of MSN_{per} . On the other hand, for Sl_{per} and SSN_{per} , it was clear that in

case when these two fractions were dominant - E_{max} decreased, which was expected, since overburden with dominant small (fine) grained particles had lower resistivity to cutting, and, thus, required lower energy consumption. As for the effect of cohesion, one could see the clear negative effect of cohesion, which was rather unexpected, but it could be explained in correspondence with the influence of Sl_{per} and SSN_{per} , i.e. increase of cohesion denoted the increase of small grained material, which further affect the decrease of E_{max} .

Regarding the significant two-factor interactions, performed analysis indicated that shear strength and grain size fractions entered the significant two factor interactions. For lower values of friction angle increase of cohesion led to decrease of E_{max} (Figure 3e). On the other hand, for higher values of ϕ , increase of cohesion did not have any significant effect on E_{max} . As for the coefficient of c and CL_{per} , it was clear from Figure 3(b) that for low clay fraction, increase of cohesion led to

decrease of E_{max} , which could be explained by the increased content of small grained sand particles, corresponding well to the interaction of CL_{per} and SSN_{per} (Figure 3a). Qualitatively similar interaction was observed for cohesion and silt percentage (Figure 3c). Co-effect of MSN_{per} and friction angle was twofold. In particular, for low values of MSN_{per} , increase of friction angle led to decrease of E_{max} , which corresponded to the overburden with lower cohesion, as shown in Figure 3(e). For higher values of MSN_{per} , increase of ϕ led to increase of E_{max} , indicating the probable increase of coarse-grained fraction. As for the interaction of CL_{per} and SSN_{per} , increase of SSN_{per} up to 50% enabled the increase of E_{max} (where coarse-grained fraction was dominant), while E_{max} decreased for fraction of SSN_{per} higher than 50% (where small grained sand and silty fraction was dominant).

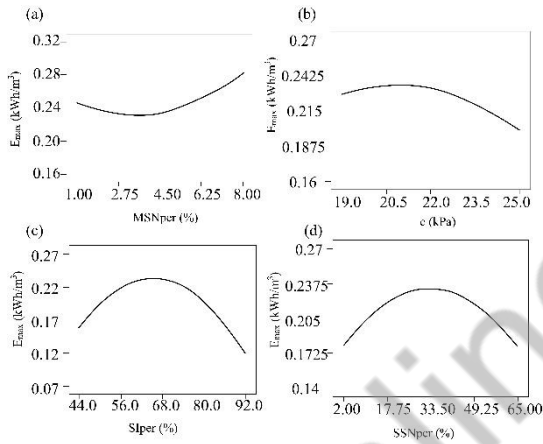


Figure 2 Statistically significant impact of individual factors MSN_{per} , SSN_{per} , Sl_{per} and c on E_{max} : (a) $E_{max}=f(MSN_{per})$, (b) $E_{max}=f(c)$, (c) $E_{max}=f(Sl_{per})$, (d) $E_{max}=f(SSN_{per})$. While a single parameter was varied, other parameters were held constant at the following values: $CL_{per}=25\%$, $Sl_{per}=67\%$, $SSN_{per}=31.5\%$, $MSN_{per}=4.5\%$, $G=19 \text{ kN/m}^3$, $c=22\text{kPa}$, $\phi=22.5^\circ$

The effect of individual factors on the cutting resistance was the following: Increase of friction angle led to decrease of cutting resistance, implying lower resistance of overburden with lower cohesion and higher friction angle (Figure 4d); On the other hand, the increase of unit weight enabled the increase of cutting resistance, which was in relation to higher compressive strength for samples with higher unit weight (Figure 4c); Impact of small-grained silty and clayey fraction is similar (Figure 4a and 4b); Increase of small-grained fraction up to the moderate values of the examined ranges led to the increase of cutting resistance,

indicating the significant fraction of coarse-grained fraction; and further increase of small-grained particles led to decrease of K_{Lmax} .

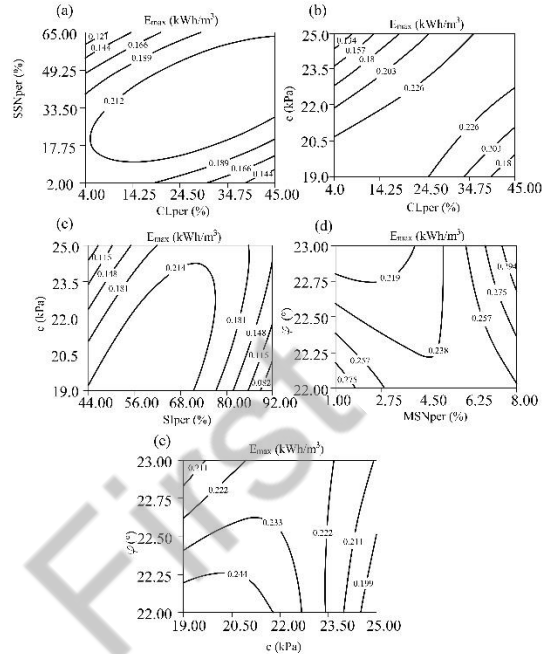


Figure 3 Statistically significant impact of two-factor interactions on E_{max} : (a) $E_{max}=f(SSN_{per} \times CL_{per})$, (b) $E_{max}=f(c \times CL_{per})$, (c) $E_{max}=f(c \times Sl_{per})$, (d) $E_{max}=f(\phi \times MSN_{per})$, (e) $E_{max}=f(\phi \times c)$. While a single parameter is varied, other parameters are being held constant at the following values: $CL_{per}=25\%$, $Sl_{per}=67\%$, $SSN_{per}=31.5\%$, $MSN_{per}=4.5\%$, $G=19 \text{ kN/m}^3$, $c=22\text{kPa}$, $\phi=22.5^\circ$

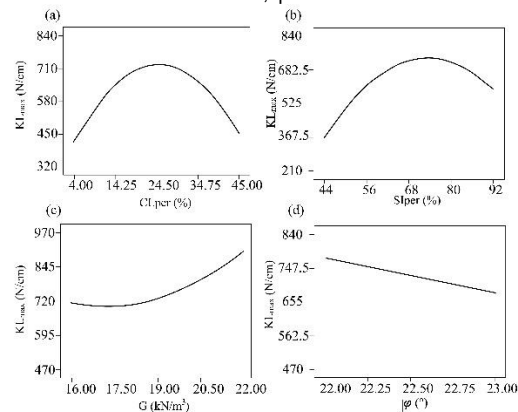


Figure 4 Statistically significant impact of individual factors CL_{per} , Sl_{per} , G and ϕ on K_{Lmax} : (a) $K_{Lmax}=f(CL_{per})$, (b) $K_{Lmax}=f(Sl_{per})$, (c) $K_{Lmax}=f(G)$, (d) $K_{Lmax}=f(\phi)$. While a single parameter is varied, other parameters are being held constant at the following values: $CL_{per}=25\%$, $Sl_{per}=67\%$, $SSN_{per}=31.5\%$, $MSN_{per}=4.5\%$, $G=19 \text{ kN/m}^3$, $c=22\text{kPa}$, $\phi=22.5^\circ$

Regarding the two-factor interactions, cohesion entered the significant two-factor interaction with all the examined grain size fractions. For low values of CL_{per} , increase of cohesion led to decrease of K_{Lmax} , indicating increasing percentage of silty fraction. For higher values of CL_{per} , increase of cohesion had almost insignificant impact on K_{Lmax} (Figure 5a). Qualitatively similar effect was observed for the co-action of c and MSN_{per} (Figure 5b) and c and Sl_{per} (Figure 5c). As for the interaction of c and SSN_{per} , for lower values of SSN_{per} , increase of cohesion had almost insignificant effect on K_{Lmax} , which corresponded well with the high percentage of CL_{per} , Sl_{per} or MSN_{per} (Figures 5a, b, c). For high values of SSN_{per} , increase of cohesion led to decrease of K_{Lmax} , which corresponded well to the low fraction of CL_{per} , MSN_{per} and Sl_{per} (Figures 5a, b, c).

Regarding the significant two-factor interactions that friction angle enters, in contrast to cohesion, φ did not enter in significant co-action with Sl_{per} , and it showed the significant co-effect with unit weight. The co-effect of φ and CL_{per} was qualitatively the same as for c and CL_{per} – for low values of CL_{per} , increase of friction angle led to decrease of K_{Lmax} . For higher values of CL_{per} , increase of φ did not have significant effect on K_{Lmax} (Figure 6b). Such insignificant effect was also observed for low values of SSN_{per} , while for higher values of SSN_{per} , increase of friction angle led to decrease of K_{Lmax} (Figure 6c). As for the co-effect of MSN_{per} and friction angle, for low values of MSN_{per} – increase of friction angle enabled the decrease of E_{max} (Figure 6b), which corresponded well to the higher percentage of SSN_{per} (Figure 6c). For higher values of MSN_{per} , increase of friction angle led to increase of K_{Lmax} , indicating higher percentage of coarse-grained fractions. Regarding the co-effect of friction angle and unit weight, for lower values of unit weight increase of friction angle led to decrease of K_{Lmax} , indicating higher percentage of small-grained particles, which had lower value of compressive strength (Figure 6a). For higher values of unit weight, increase of friction angle had almost insignificant effect on K_{Lmax} .

As for other significant two-factor interactions, the obtained results indicated that for low values of CL_{per} , increase of Sl_{per} led to increase of K_{Lmax} , which could be ascribed to lower cohesion of silty particles compared to cohesion between clay particles (Figure 7a). Almost insignificant effect of the increase of Sl_{per} on K_{Lmax} was obtained for higher values of CL_{per} . Regarding the co-effect of unit weight and CL_{per} , for the lowest values of CL_{per} , increase of unit weight had almost insignificant effect on K_{Lmax} (Figure 7b). For the

moderate and high values of CL_{per} , increase of unit weight caused the increase of K_{Lmax} , indicating samples of overburden with higher compressive strength. As for the co-effect of Sl_{per} and MSN_{per} , increase of Sl_{per} for almost all examined values of MSN_{per} enabled the increase of K_{Lmax} , which was connected with higher cohesion among silty particles compared to medium-grained sand particles (Figure 7c).

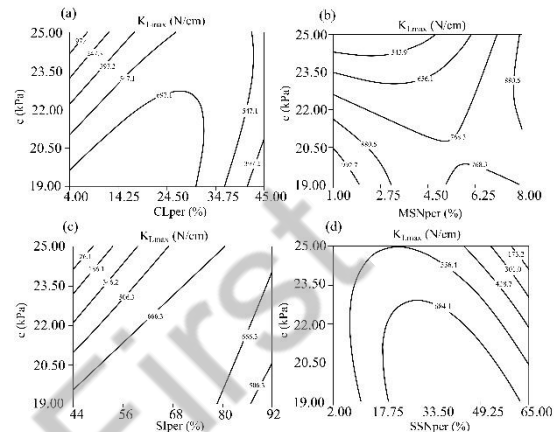


Figure 5 Statistically significant impact of two-factor interactions: cohesion c and grain size fractions on K_{Lmax} : (a) $K_{Lmax}=f(c \times CL_{per})$, (b) $K_{Lmax}=f(c \times MSN_{per})$, (c) $K_{Lmax}=f(c \times Sl_{per})$, (d) $K_{Lmax}=f(c \times SSN_{per})$. While a single parameter is varied, other parameters are being held constant at the following values: $CL_{per}=25\%$, $Sl_{per}=67\%$, $SSN_{per}=31.5\%$, $MSN_{per}=4.5\%$, $G=19 \text{ kN/m}^3$, $c=22 \text{ kPa}$, $\varphi=22.5^\circ$

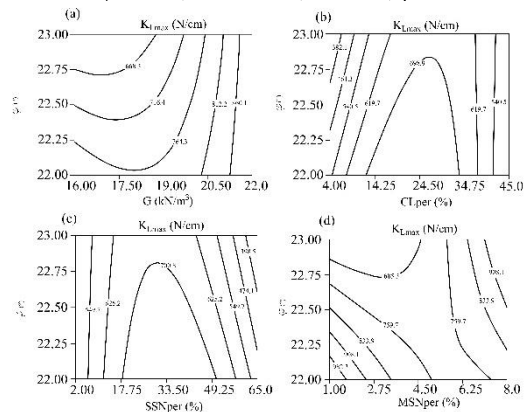


Figure 6 Statistically significant impact of two-factor interactions: angle of internal friction φ , grain size fractions and unit weight on K_{Lmax} : (a) $K_{Lmax}=f(\varphi \times G)$, (b) $K_{Lmax}=f(\varphi \times CL_{per})$, (c) $K_{Lmax}=f(\varphi \times SSN_{per})$, (d) $K_{Lmax}=f(\varphi \times MSN_{per})$. While a single parameter is varied, other parameters are being held constant at the following values: $CL_{per}=25\%$, $Sl_{per}=67\%$, $SSN_{per}=31.5\%$, $MSN_{per}=4.5\%$, $G=19 \text{ kN/m}^3$, $c=22 \text{ kPa}$, $\varphi=22.5^\circ$

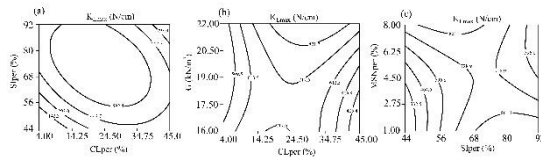


Figure 7 Statistically significant impact of two-factor interactions: grain size fractions and unit weight on K_{Lmax} : (a) $K_{Lmax}=f(SI_{per} \times CL_{per})$, (b) $K_{Lmax}=f(G \times CL_{per})$, (c) $K_{Lmax}=f(SI_{per} \times MSN_{per})$. While a single parameter is varied, other parameters are being held constant at the following values: $CL_{per}=25\%$, $SI_{per}=67\%$, $SSN_{per}=31.5\%$, $MSN_{per}=4.5\%$, $G=19 \text{ kN/m}^3$, $c=22 \text{ kPa}$, $\varphi=22.5^\circ$

4. Conclusions

The multiple linear regression analysis was discussed in this paper in order to examine the effect of different physical and mechanical parameters of overburden on the excavator energy consumption and maximum linear cutting resistance. Data used for analysis was recorded at "Tamnava Eastern field" surface mine [16]. The obtained results indicated the following:

- Overburden unit weight had no statistically significant effect on the excavator maximum energy consumption. Regarding the maximum linear cutting resistance, it had significant positive impact on K_{Lmax} , and it entered statistically significant two-factor interactions with friction angle and CL_{per} . Strong individual positive impact of G on K_{Lmax} could be explained by the higher compressive strength of samples with higher unit weight. This same positive effect of G and K_{Lmax} remained for all values of friction angle and CL_{per} .
- Clay fraction percentage in overburden had no statistically significant individual effect on E_{max} , but it entered into significant two-factor interactions with cohesion and small-grained sand fraction. In general, E_{max} decreased with the increase of CL_{per} , for approximately any value of SSN_{per} or cohesion. As for the effect on K_{Lmax} , there was a parabolic change of K_{Lmax} with the increase of CL_{per} . This indicated that low fraction of clay particles in overburden did not have significant effect on K_{Lmax} , up to approx. 24.5 %. Regarding the two-factor interactions, CL_{per} entered two-factor interaction with cohesion, friction angle, unit weight, and silt percentage. Decrease of E_{max} for $CL_{per} > 24.5\%$

was also observed in these cases, regardless of the values c , φ and SI_{per} .

- Silt fraction percentage in overburden had significant individual effect on E_{max} , but only when it represented dominant fraction; in present case, after 68%. Also, it entered statistically significant two factor interaction with cohesion, where it also led to decrease of E_{max} after 68% regardless of the cohesion. Qualitatively similar individual effect SI_{per} has on K_{Lmax} . As for the significant two-factor interactions, it also entered the significant interaction with cohesion (qualitatively the same as for E_{max}), CL_{per} and MSN_{per} .
- Small-grained sand fraction percentage in overburden had qualitatively the same individual effect on E_{max} , as silt percentage, only for the values higher than 33%. As for the two-factor interaction, SSN_{per} entered the interaction with CL_{per} , where the increase of SSN_{per} led to decrease of E_{max} , regardless of CL_{per} . SSN_{per} did not show significant effect on K_{Lmax} . Regarding the significant two-factor interactions, SSN_{per} showed significant interactions both with cohesion and friction angle. Increase of SSN_{per} led to decrease of K_{Lmax} regardless of cohesion, while this effect was observed in the interaction with friction angle for $SSN_{per} > 33\%$.
- Increase of moderate-grained sand fraction percentage led to increase of E_{max} , indicating higher resistance to cutting. This effect was also shown in significant two-factor interaction with friction angle. MSN_{per} had no significant individual effect on K_{Lmax} , while it entered statistically significant interaction with cohesion. In this case, for lower values of cohesion, effect of MSN_{per} on K_{Lmax} was almost insignificant, while increase of MSN_{per} for stronger cohesion led to increase of K_{Lmax} . MSN_{per} also entered significant interaction with SI_{per} , where for low values of SI_{per} , increase of MNS_{per} led to increase of E_{max} , while its effect was negligible for higher values of SI_{per} .
- Increase of overburden cohesion led to decrease of E_{max} , which was also observed in the interaction with friction angle, CL_{per} and SI_{per} . Cohesion showed no statistically significant individual effect on K_{Lmax} , while it entered in statistically significant two-factor interactions with SSN_{per} , CL_{per} , SI_{per} and MSN_{per} ,

where it showed qualitatively similar influence, regarding of the SSN_{per} , CL_{per} , SI_{per} and MSN_{per} .

- Overburden friction angle showed no statistically significant individual effect on E_{max} , while it entered in the significant interaction with cohesion and MSN_{per} , where it generally exhibited negative effect. Regarding the effect on K_{Lmax} , ϕ showed significant negative individual effect on K_{Lmax} , while it also entered significant two-factor interactions with unit weight, CL_{per} , MSN_{per} and SSN_{per} . In all these interactions, increase of friction angle led to decrease of K_{Lmax} , except for the highest values of CL_{per} and MSN_{per} , where positive effect was observed.

One should note that the results obtained in presented research could be directly used at the specific site for which they are obtained, or for the coal sites with the same or similar geotechnical conditions. In other cases, presented research could serve as a methodological guidance for defining new site-specific estimation models.

Further research on this topic could include the wider range of values of the examined parameters, especially MSN_{per} and friction angle. Also, other mechanical parameters could be included, like compressibility modulus or uniaxial compressive strength.

5. References

- [1] Ulbrich, D., Selech, J., Romek, D., Sieńkowski, M., Włodarczyk, K., Kowalczyk, J., Staszak, Z., Marcinkiewicz, J. (2018) Analysis of the costs of regeneration of excavator buckets used for brown coal excavation. *Journal of Research and Applications in Agricultural Engineering* 63(1), 135-139.
- [2] Lakshminarayana, C.R., Tripathi, A.K., Pal, S.K. (2021) Experimental investigation on potential use of drilling parameters to quantify rock strength. *International Journal of Geo-Engineering* 12(1), 23: 1-15.
- [3] Shreyas, S.K., Dey, A. (2019) Application of soft computing techniques in tunnelling and underground excavations: state of the art and future prospects. *Innovative Infrastructure Solutions* 4(1), 46: 1-15.
- [4] Kumar, C., Kumaraswamidhas, L.A., Murthy, V.M.S.R., Prakash, A. (2020) Experimental investigations on thermal behavior during pick-rock interaction and optimization of operating parameters of surface miner. *International Journal of Rock Mechanics and Mining Sciences* 133,104360, 1-11.
- [5] Zhang, Q., Yang, K., Wang, L., Zhou, S. (2020) Geological Type Recognition by Machine Learning on In-Situ Data of EPB Tunnel Boring Machines, *Mathematical Problems in Engineering* 3057893, 1-10.
- [6] Mohamad E.T. Koopialipoor M., Murlidhar B.R. Rashid A., Hedayat A., Jahed Armaghani D. (2019) A new hybrid method for predicting ripping production in different weathering zones through in situ tests. *Measurement: Journal of the International Measurement Confederation* 147,106826.
- [7] Trivan, J. (2021) Complex study of excavation resistance for application of cross-pit spreader system in conditions of hard rock masses at surface mines. PhD thesis. University of Banja Luka Faculty of Mining Prijedor, pp. 121.
- [8] Coleman, J.R., Fitzhardinge, C.F.R. (1979) Geotechnology of excavation equipment selection with particular emphasis on bucket wheel excavators, *Proc. Int. Conf. on Mining and Machinery, Inst. Engineers, Australia, Brisbane, Australia*, 139-146 str.
- [9] Inal, A. (1984) The development of a diggability index for bucket wheel excavators. The University of New South Wales School of Mining Engineering Faculty of Applied Science, Master work, pp 167.
- [10] Scheffler, D. (1997) Laboratory and in-situ methods of measurement as the basis for predicting cutting resistances in mining machines. *ZKG International* 50 (7), 347-352. str.
- [11] Razz, V. (1999) Assessment of the Digging Force and optimum selection of the and Operational parameters of Bucket Wheel Excavators for mining of Overburden Coal and partings, Braunkohle, Krupp Fördertechnik GmbH: Essen, Germany
- [12] Su, O., Akcin, N.A. (2005) Investigation of the relationships between Cerchar hardness index and some index properties of coal. *Proceedings of the 19th International Mining Congress and fair of Turkey, IMCET2005*, 1-5 str.
- [13] Amar, P., Vemavarapu, M., Ramachandra, M.S., Bahadur, S.K. (2013) Rock excavation using surface miners: An overview of some design and

- operational aspects. International Journal of Mining Science and Technology, 23, 33–40 str.
- [14] Langham-Williams, J., Hagan, P. (2014) An assessment of the correlation between the strength and cuttability of rock. Proceedings of the 14th Coal Operators' Conference, University of Wollongong, The Australian Institute of Mining and Metallurgy & Mine Managers Association of Australia, 186-192.
- [15] Kostić, S., Trivan, J. (2022) Optimization of coal overburden excavation considering variable geomechanical properties and states of excavator teeth, Archives of Mining Sciences 67 (in print)
- [16] Ignjatović, D. (2003) Study on optimization of excavator bucket construction for increasing of capacity. University of Belgrade Faculty of Mining and Geology, pp 218 (in Serbian).

PROCENA POTROŠNJE ENERGIJE BAGERA I OTPORNOSTI NA REZANJE OTKRIVKE KORIŠĆENJEM VIŠESTRUKNE LINEARNE REGRESIJE

J. Trivan¹, S. Kostić^{2#}

¹University of Banja Luka, Faculty of Mining, Prijedor, Republic of Srpska, Bosnia and Herzegovina

²Jaroslav Černi Water Institute, Geology Department, Belgrade, Serbia

Primljen: 15. mart 2022.; Prihvaćen: 20. oktobar 2022.

Izvod

U ovom radu su ispitani potrošnja energije bagera i linearni otpor na rezanje otkrivke. Kao rezultat istraživanja, predloženi su odgovarajući modeli kao nelinearne funkcije fizičkih i mehaničkih svojstava otkrivke: veličina zrna, specifična težina, kohezija i ugao trenja. Analiza je izvršena na osnovu podataka prikupljenih na kopu „Tamnava – Istočno polje“ za rotorni bager sa novim zupcima za otkopavanje. Dobijeni rezultati su pokazali da potrošnja energije bagera značajno zavisi od veličine zrna i kohezije kao pojedinačnih faktora, a značajan uticaj je imala i dvofaktorska interakcija: procenat gline sa kohezijom i sitnozrnastom frakcijom peska, kao i ugao trenja sa srednjezrnastim peskom i kohezijom. S druge strane, linearna otpornost otkrivke na rezanje je u velikoj meri kontrolisana svim ispitivanim fizičko-mehaničkim svojstvima (veličinom zrna, specifičnom težinom i čvrstoćom na smicanje), uz sledeće značajne dvofaktorske interakcije: parametri čvrstoće na smicanje sa svim veličinama frakcija, međusobne frakcije sa različitim veličinama zrna i ugao trenja sa specifičnom težinom.

Ključne reči: Otpornost na rezanje; Potrošnja energije; Specifična težina; Veličina zrna; Čvrstoća na smicanje; Višestruka linearna regresija.